

GEOPHYSICAL MODEL APPLICATIONS FOR MONITORING

Michael E. Pasyanos, William R. Walter, Hrvoje Tkalčić,
Gregory A. Franz, Rengin Gök, and Arthur J. Rodgers

Lawrence Livermore National Laboratory

Sponsored by National Nuclear Security Administration
Office of Nonproliferation Research and Engineering
Office of Defense Nuclear Nonproliferation

Contract No. W-7405-ENG-48

ABSTRACT

Geophysical models constitute an important component of calibration for nuclear explosion monitoring. We will focus on four major topics and their applications: 1) surface wave models, 2) receiver function profiles, 3) regional tomography models, and 4) stochastic geophysical models. First, we continue to improve upon our surface wave model by adding more paths. This has allowed us to expand the region to all of Eurasia and into Africa, increase the resolution of our model, and extend results to even shorter periods (7 sec). High-resolution models exist for the Middle East and the Yellow Sea and Korean Peninsula (YSKP) region. The surface wave results can be inverted either alone, or in conjunction with other data, to derive models of the crust and upper mantle structure. One application of the group velocities is to construct phase-matched filters in combination with regional surface-wave magnitude formulas to improve the mb:Ms discriminant and extend it to smaller magnitude events. Next, we are using receiver functions, in joint inversions with the surface waves, to produce profiles directly under seismic stations throughout the region. In the past year, we have been focusing on deployments throughout the Middle East, including the Arabian Peninsula and Turkey. By assembling the results from many stations, we can see how regional seismic phases are affected by complicated upper mantle structure, including lithospheric thickness and anisotropy. The next geophysical model item, regional tomography models, can be used to predict regional travel times such as Pn and Sn. The times derived by the models can be a background model for empirical measurements or, where these don't exist, simply used as is. Finally, we have been exploring methodologies such as Markov Chain Monte Carlo (MCMC) to generate data-driven stochastic models. We have applied this technique to the YSKP region using surface-wave dispersion data, body wave travel time data, receiver functions, and gravity data. The models can be used to predict a number of geophysical measurements, including waveforms that can be generated using techniques such as finite difference and spectral element modeling.

OBJECTIVE

The objective of regional-scale geophysical models is to improve predictions for the location and identification of regional seismic events by improving the resolution in comparison to global-scale models. As such, we wish to provide models of the highest possible resolution that can be used to reliably derive parameters such as body wave travel times, group velocity dispersion, waveforms, etc. In addition, the models should convey proper uncertainty estimates which can be mapped into uncertainties in the derived products.

Geophysical models can take a number of forms. Much interest in *a priori* models has been made in the monitoring community in recent years and several of them have been constructed by various groups for different regions. Examples include the WINPAK model (Johnson and Vincent, 2002) for India and Pakistan, the WENA model (Pasyanos et al., 2004) for Western Eurasia and North Africa, as well as the various consortia models. These models can serve as background values for travel time correction surfaces and other derived parameters. This can be particularly important in aseismic regions, which might only have a limited number of empirical measurements. These models can also serve as an integrated geophysical repository for research community results.

In this paper, however, we will not be discussing *a priori* geophysical models, but rather concentrate on several other types of geophysical models. The focus in this paper is to outline some of the other model types, and focus as much as possible on their applications to monitoring. The first that we consider are surface-wave models. By themselves, these stand-alone models can be used to construct phase-matched filters, which can improve weak surface wave signal and calculate regionally determined M_s . In addition, they can be used either alone or in conjunction with other data to construct 3-D velocity models of the lithosphere. A second type is receiver functions, which are a reliable way of obtaining the local velocity structure near a station from teleseismic events. While the results are only applicable to the limited portions of our model area covered by seismic stations, they are important to constrain precisely because they represent the structure at the station locations. Regional tomography models, such as those for upper mantle head-waves P_n and S_n , can be used to predict regional travel times. We present our results from stochastic models, which are data-driven models generated using a Markov Chain Monte Carlo (MCMC) technique. This method combines a priori information with geophysical data from multiple sources (and varying sensitivities) to produce models that are most consistent with the constraints. Finally, all of the methods can be used to evaluate some of the aforementioned *a priori* geophysical models.

RESEARCH ACCOMPLISHED

Surface Wave Models

Over the past several years, Lawrence Livermore National Laboratory (LLNL) has been developing surface wave models in Eurasia for nuclear explosion monitoring (Pasyanos et al., 2001; Pasyanos, 2005). Dispersion measurements are made using multiple narrow-band filters on deconvolved displacement data from the LLNL Seismic Research Knowledge Base (SRKB). We continue to improve upon our surface wave model by adding more paths, generally by taking advantage of new data sets, but also by revisiting stations with more recent events. Most recently, we have added measurements from stations in Eastern Europe, Central Asia, Africa, and the Indian Ocean, including several the Incorporated Research Institutions for Seismology program that manages seismic equipment (PASSCAL) deployments.

To date, over 100,000 seismograms have been analyzed to determine the individual group velocities of 7-150 second Rayleigh and Love waves. Overall, we have made good quality dispersion measurements for 30,000 Rayleigh and 20,000 Love wave paths. We then tomographically invert these measurements to produce group velocity maps for Love and Rayleigh waves. A conjugate gradient method is used for the tomography.

27th Seismic Research Review: Ground-Based Nuclear Explosion Monitoring Technologies

The group velocity models continue to improve in several ways. First, with more measurements, we have been able to expand the region of coverage to all of Eurasia and into Africa. By increasing the density of coverage in existing regions, we have increased the resolution of our model. Finally, we have been able to provide more reliable maps at short periods, expanding the frequency coverage down to a 7-second period. With the group velocities, we are able to resolve structural features associated with the tectonics of the region. Short period surface waves correspond well to sedimentary basins. At intermediate periods, we find a good correspondence to crustal thickness, but still see the effect of the deepest sedimentary basins. At long periods, we are primarily sensitive to upper mantle structure with fast cratons, slow convergence zones, and very slow ridges (Pasyanos, 2005).

Path coverage will be further improved in the future by the use of cross-correlation of ambient seismic noise to derive the Green function between two stations, and from which the dispersion characteristics can be derived. The benefits of this method in seismology have been dramatically demonstrated for southern California in Shapiro et al. (2005). Figure 1 shows cross-correlations from stations in the eastern Mediterranean using only one month of data. Even with this limited data, the Rayleigh wave signal is already starting to emerge and will become clearer as more data are stacked.

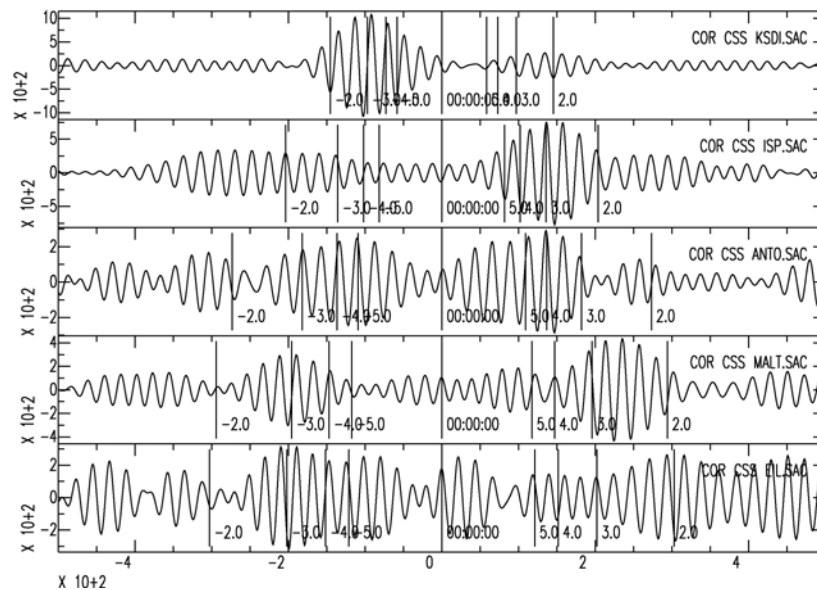


Figure 1. Cross-correlation waveforms between station CSS (Cyprus) and nearby stations KSDI (Kfar Sold, Israel), ISP (Isparta, Turkey), ANTO (Ankara, Turkey), MALT (Malatya, Turkey), and EIL (Eilat, Israel) between 20 and 25 secs derived from one month of data.

We have created high-resolution models for the Middle East and the YSKP region (Pasyanos, 2005). Figure 2 shows an example of our results from the Middle East for 15 second Rayleigh waves, which are sensitive to relatively shallow crustal structure. Here, we compare the results to a sediment thickness map and the results are excellent. Details like the extent of basins in the eastern Mediterranean, Persian Gulf, Mesopotamian Foredeep, and Caspian Sea are well resolved, as is the thin oceanic crust in the Red Sea.

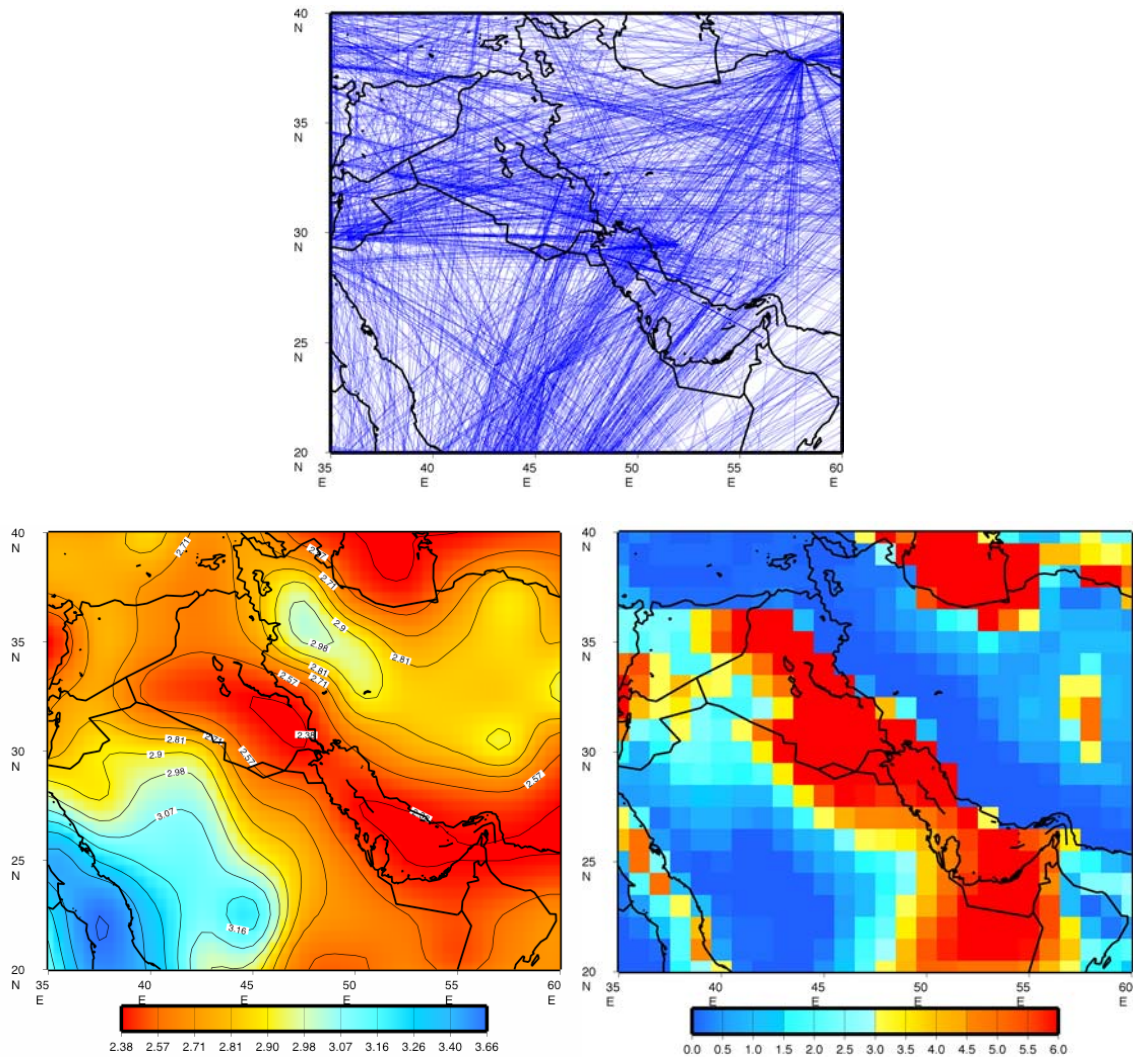


Figure 2. A path map of 15-second Rayleigh wave group velocities for the Middle East, followed by a tomographic model of 15-second Rayleigh waves and a comparison of the results to a sediment thickness map of the region (Laske and Masters, 1997). The color bar scale for the left figure is km/s (group velocity). The scale for the right figure is km (sediment thickness).

The surface wave results can be inverted either alone, or in conjunction with other data, to derive models of the local crust and upper mantle structure. By combining the surface wave data with other data, we can reduce the non-uniqueness inherent in the profile inversions performed using only surface wave data. In the next section, for example, we will be using the surface-wave data in combination with teleseismic receiver functions.

Another application of the group velocities is to construct phase-matched filters in combination with regional surface-wave magnitude formulas to improve the mb:Ms discriminant and extend it to smaller magnitude events. Phase-matched filtering has been shown to effectively winnow out any unwanted signals from the surface wave signal. An example of phase matched filtering is shown in Figure 3. The first example is from an event in eastern Turkey recorded at station HILS in Saudi Arabia. The top figure shows the original trace which shows body phases Pn and Pg, followed by a very large Lg phase coming in at a group velocity of about 3.5 km/s. The main surface-wave energy is followed by a second packet of surface

waves, and followed until the end of the trace by coda. The second trace shows the same event after the waveform has been phase-matched filtered using the tomography of Pasyanos (2005). The body waves including the large Lg phase are completely removed. In addition, the late-arriving multipathed surface waves are beaten down, as is the coda. This is a particularly good example of how using a phase-matched filter can improve our signal. The maximum amplitude surface wave without the filter would be energy arriving at 2.4 km/s, rather than the direct signal at 2.8 km/s. The bottom trace shows the residual signal that was filtered out by the phase-matched filter. Regional surface-wave magnitudes calculated using narrow-band filters (Russell, 2004) from the cleaned signal show a more consistent magnitude value between periods.

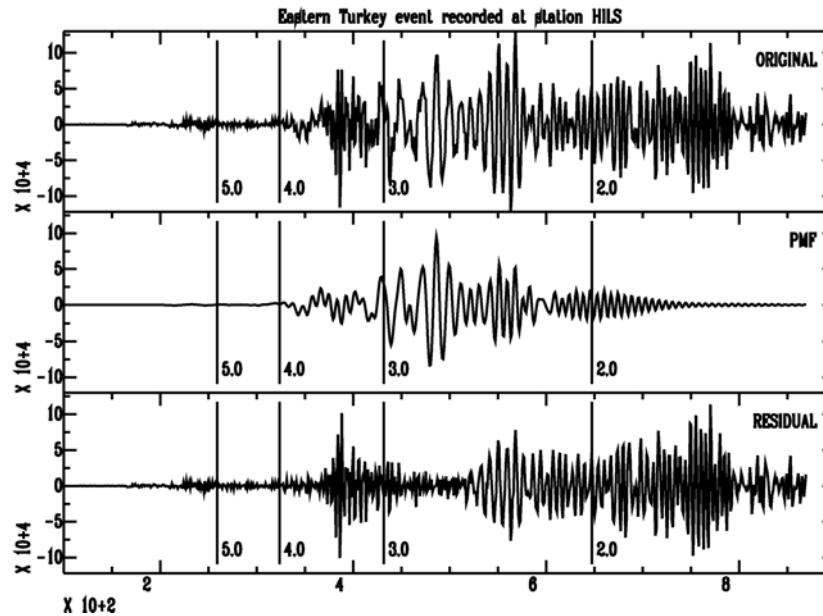


Figure 3. Waveform of an event in eastern Turkey recorded at station HILS in Saudi Arabia. The top trace shows the original waveform, the middle trace shows the waveform filtered using a phase-matched filter from the model of Pasyanos (2005), and the bottom trace shows the residual.

Receiver Function Profiles

We are also using receiver functions, in joint inversions with the surface waves, to produce profiles directly under seismic stations throughout the region. These two data types are complementary since receiver functions are sensitive to velocity contrasts and surface waves are sensitive to depth-averaged velocity. In a collaborative ROA with Penn State University, Ammon et al. have been focusing on stations throughout Western Eurasia and North Africa, while we have been focusing on Livermore deployments and cooperative ventures in the Middle East, including Kuwait, Jordan, Saudi Arabia, and the United Arab Emirates.

An example of a joint inversion is shown for station KBRS in Saudi Arabia. This station was selected as an example of a station which has a simple crustal but a complex lithospheric structure, resulting in models that cannot fit jointly the observed receiver functions and surface-wave group velocity dispersion curves. In this case, in order to produce realistic models that simultaneously fit the surface waves (both Love and Rayleigh) without significantly degrading the fit to the receiver functions, we need to introduce a more complicated upper mantle structure, having both lithospheric structure and anisotropy. The final model and fits to the teleseismic receiver functions and surface wave group velocity dispersion data are shown in Figure 4. A gradational Moho between 35 and 38 km is found in our best model. It was then necessary to

introduce a thin lithospheric lid and a low velocity zone in the upper mantle in order to match low velocities observed in the group velocity dispersion. A strong transverse isotropy (with $SH > SV$) is required in the upper mantle below Moho down to about 70-80 km in order to fit longer periods of Rayleigh wave group velocity dispersion. The profiles are also consistent with the tectonic setting of the region. In this region of the Arabian Peninsula, we find the thin sedimentary cover that would be expected for the Arabian Shield, a moderately thick crust, a lid indicating a 70 km thickness lithosphere over an asthenosphere with significantly slower shear wave velocity, and anisotropy consistent with mantle material laterally spreading away from the Red Sea Rift.

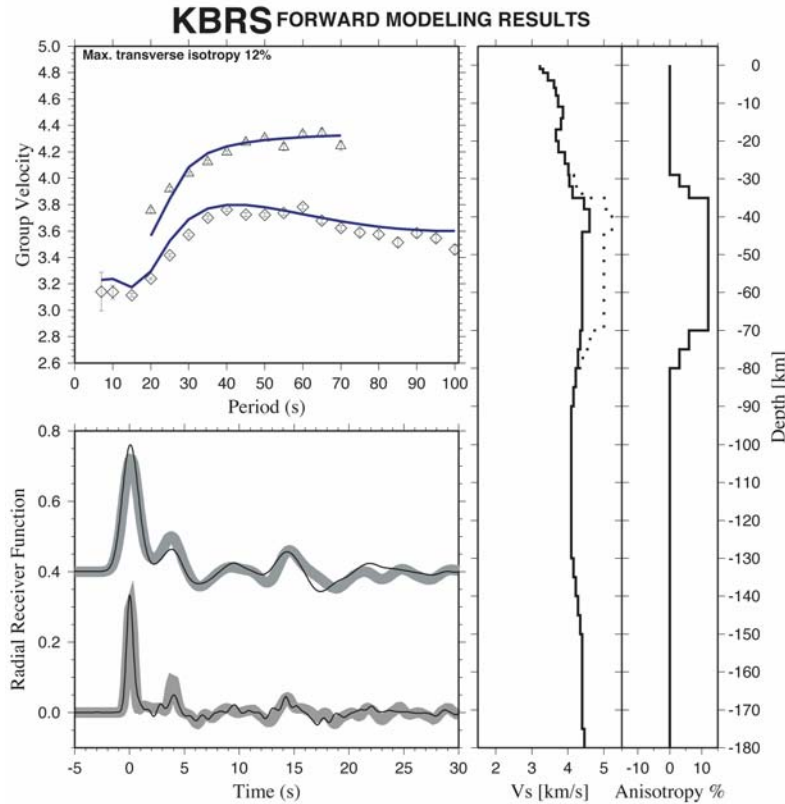


Figure 4. Joint inversion of receiver functions and surface waves to produce a velocity profile for station KBRs in Saudi Arabia. Upper left: symbols are surface-wave group velocity data points derived from surface-wave tomography, and solid lines represent a modeled dispersion. Lower left: Thick lines represent the observed receiver functions at two distinct frequency bands (for Gaussian parameter $a=1.0$ (top) and $a=2.5$ (bottom)), while thin solid lines are modeled receiver functions from the model shown on right. Right: final model of shear wave velocity as a function of depth. The dotted line shows V_{sh} where it differs from V_{sv} .

Regional Tomography Models

Regional tomography models can be used to predict the travel times of regional phases such as P_n and S_n . While details of the various methodologies vary, they all generally tomographically distribute the slowness along the upper mantle leg of the path, while either inverting or making some sort of correction for the crustal legs. The advantages of such a method is that the tomography can be used to help estimate travel times of these regional phases, even when no direct measurements have been made at a particular station. Due to the propagation path of these phases, however, the spatial coverage is generally limited to a relatively narrow swath around seismic areas within about 1500 km from events, making it of limited use in

aseismic regions. Another potential problem is that normalization in the tomography can dampen the full amplitude of the velocity anomalies.

Still, the utility of tomography is evident. A comparison of P-wave velocities in the upper mantle from both an *a priori* model and tomographic inversion is shown in Figure 5. While the two models generally show the same features (fast velocities beneath oceans, India, and the Former Soviet Union; slow beneath Red Sea, East African Rift, Tethys Belt; sharp contrast along the TTZ), there are obvious differences. Most notably, besides about a 0.04 km/s shift between the two models, there is considerable unmodeled variation in the tomography which does not exist in the *a priori* model. It is this variability that would be difficult to build into a *a priori* type models. The application of these models, of course, is to predict these regional phases. The times derived by the models can be as a background model for empirical measurements or, where these don't exist, simply used as is.

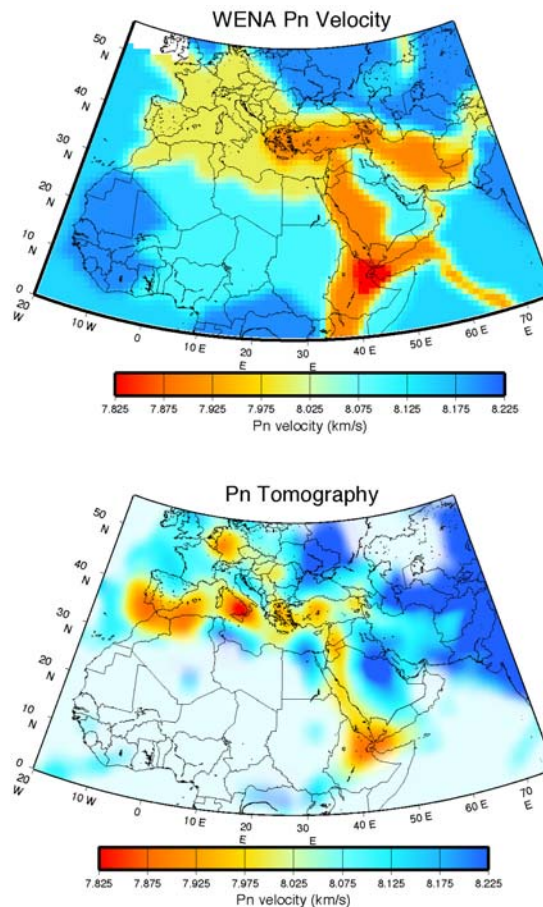


Figure 5. A comparison of uppermost mantle P-wave velocities from an *a priori* model and tomographic inversion. (a) The upper mantle velocities predicted by the WENA model. (b) The upper mantle velocities derived from the Pn tomography (Pasyanos et al., 2004).

Stochastic Geophysical Models

We have been exploring methodologies such as MCMC to generate data-driven stochastic models. In an effort to build seismic models that are most consistent with multiple seismic data sets, we have applied a new method known as the Stochastic Engine (SE). The SE uses MCMC to sample models from a prior distribution and test them against multiple data types in a staged approach to generate a posterior distribution of models.

While computationally expensive, this approach has several advantages over a single deterministic model. First, we are able to easily incorporate prior information on the model, such as the *a priori* geophysical models that were discussed earlier. Second, with this technique, we are able to reconcile different data types that can be used to constrain the model. We can also estimate the uncertainties of model parameters, properly migrating data uncertainties into model uncertainties. The method does not constrain models to be normally distributed, but instead allows non-Gaussian or multi-modal distributions. Finally, we can estimate uncertainties on predicted observable signals, such as would be required to apply this model as a correction surface.

We use this method to determine the crust and upper mantle structure of the Yellow Sea and Korean Peninsula (YSKP) region using surface wave dispersion data, body wave travel time data, and receiver functions. We have had great success using this approach. Where little or no data exist, the posterior model simply reflects the prior distribution. Where data exists, however, the model is driven by the data. Figure 6 shows a crustal thickness map and corresponding uncertainties, taken by calculating the mean and standard deviation of the posterior distribution. One can see the thinning associated with the oceanic crust of the Pacific Ocean and Sea of Japan. One can also see crustal thickening in the westernmost portion of our study area. We are in the process of improving the model by incorporating more data sets (i.e., gravity, amplitude information, waveforms, etc.) and increasing the resolution to 1 degree.

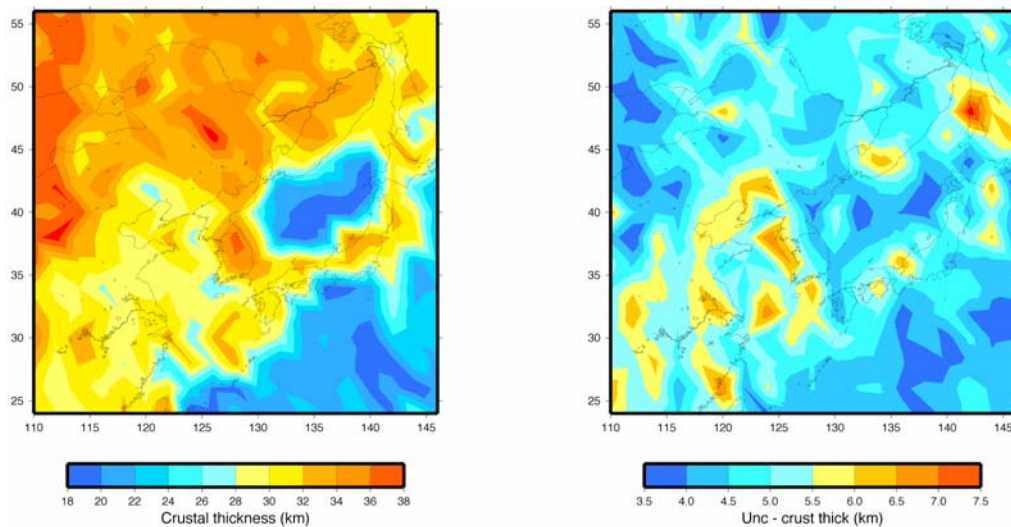


Figure 6. A crustal thickness map of the YSKP region determined using stochastic inversion methods, along with its associated uncertainties.

We also use this model to predict waveforms using a spectral element model (Komatitsch et al., 2002). Figure 7 shows a comparison of waveforms along a path from an event in the Liaodong Peninsula in China to station BJT in Beijing. Waveforms were calculated for the 1D PREM model (Dziewonski and Anderson, 1981), the CRUST2.0 (Bassin et al., 2000) model with S20RTS (Ritsema et al., 1999) mantle, the CUB2.0 model (Shapiro and Ritzwoller, 2002), and the mean MCMC model (Pasyanos et al., 2005). Unsurprisingly, the waveforms generated using the PREM model do not fit the data. The CRUST2.0 and CUB2.0 models both fit the early arrivals but neither model fits the late arriving energy. The MCMC model, however, which has thicker sediments along the profile, fits more of the waveform.

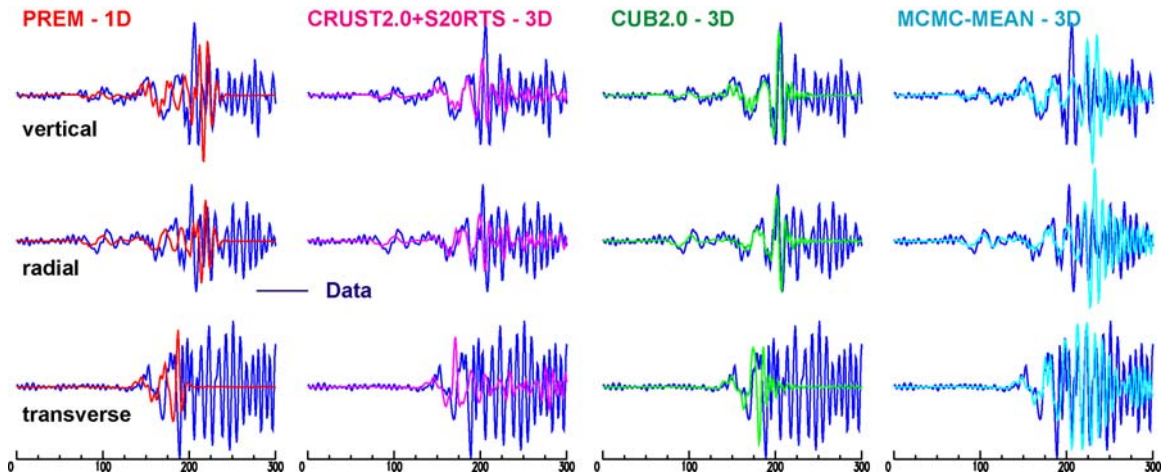


Figure 7. Waveforms for a path in eastern China generated using the spectral element method for models PREM (red), CRUST2.0 and S20RTS (magenta), CUB2.0 (green), and the MCMC method (cyan), and compared with data (blue).

In short, stochastic methods are an innovative technique for producing next-generation data-driven models. *A priori* models can be used as starting models for the inversion. Other model information such as surface wave dispersion measurements, teleseismic receiver functions, and regional body wave travel times (shown in the first three sections) can be included as additional constraints. Stochastic models have a number of advantages compared to traditional models, such as the ability to reconcile different types of geophysical data. An important component of this is the ability to predict new observables with proper uncertainties.

CONCLUSIONS AND RECOMMENDATIONS

Geophysical models are an important way of calibrating regions in the absence of direct measurements. Models can be a repository for a vast array of geological and geophysical datasets of all types—receiver functions, refraction profiles, tomographic inversions, travel time models, amplitude measurements, etc. This product integrates results from many sources and can be used to incorporate future results from current research.

Geophysical model research at LLNL has developed along a number of lines. We have developed a 3-D geophysical model for Western Eurasia and North Africa, along with sophisticated access tools, which are directly usable for generating a number of geophysical parameters of interest. The surface wave measurements and model for greater Eurasia, receiver functions throughout the region provide additional model constraints, and tomographic models can be used to predict regional travel times. We are now moving toward developing data-driven geophysical models that can use all of these results to produce reliable geophysical models.

REFERENCES

- Bassin, C., G. Laske, and G. Masters, (2000), Current limits of resolution for surface wave tomography in North America, *EOS Trans AGU* 81: F897.
- Dziewonski A.M., and Anderson D.L. (1981), Preliminary reference Earth model. *Physics of the Earth Planetary Interiors* 25: 297-356.
- Johnson, M. and C. Vincent (2002), Development and testing of a 3-D velocity model for improved event location: a case study for the India-Pakistan region, *Bull. Seism. Soc. Amer.* 92: 2893-2910.

27th Seismic Research Review: Ground-Based Nuclear Explosion Monitoring Technologies

- Komatitsch, D., J. Ritsema, J. Tromp (2002), The spectral-element method, Beowulf computing, and global seismology, *Science* 298: 1737-1742.
- Laske, G. and T.G. Masters (1997), A global digital map of sediment thickness, *EOS Trans. AGU* 78: F483.
- Pasyanos, M. E., W. R. Walter, S. E. Hazler (2001), A surface wave dispersion study of the Middle East and North Africa for monitoring the Comprehensive nuclear-test-ban Treaty, *Pure and Applied Geophysics* 158: 1445-1474.
- Pasyanos, M. E., W. R. Walter, M. P. Flanagan, P. Goldstein and J. Bhattacharyya (2004), Building and testing an a priori geophysical model for western Eurasia and North Africa, *Pure and Applied Geophysics*, 161, 235-281.
- Pasyanos, M.E. (2005), A variable-resolution surface wave dispersion study of Eurasia, North Africa, and surrounding regions, submitted to *J. Geophys. Res.*
- Pasyanos, M.E., G.A. Franz, and A.L. Ramirez (2005), Reconciling a geophysical model to data using a Markov Chain Monte Carlo algorithm: An application to the Yellow Sea – Korean Peninsula region, submitted to *J. Geophys. Res.*
- Ritsema, J., H. J. van Heijst, and J. H. Woodhouse (1999), Complex shear wave velocity structure imaged beneath Africa and Iceland, *Science* 286: 1925-1928.
- Russell, D.R. (2004), Theoretical analysis of narrow-band surface wave magnitudes, AFTAC report AFTAC-TR-04-004, 42 pp.
- Shapiro, N.M. and M.H. Ritzwoller (2002), Monte-Carlo inversion for a global shear velocity model of the crust and upper mantle, *Geophys. J. Int.* 151: 88-105, 2002.
- Shapiro, N.M., M. Campillo, L. Stehly, and M.H. Ritzwoller (2005), High resolution surface wave tomography from ambient seismic noise, *Science* 307(5715): 1615-1618.